

Density Functional Theory Study of Co, Rh, and Ir Atoms Deposited on the α -Al₂O₃(0001) Surface

N. Cruz Hernández,[†] A. Márquez,[†] J. F. Sanz,^{*,†} J. R. B. Gomes,^{‡,§} and F. Illas[§]

Departamento de Química Física, Facultad de Química, Universidad de Sevilla, E-41012 Sevilla, Spain, Centro de Investigação em Química, Faculdade de Ciências da Universidade do Porto, R. Campo Alegre, 687, 4169-007 Porto, Portugal, and Departament de Química-Física i Centre especial de Recerca en Química Teòrica, Universitat de Barcelona i Parc Científic de Barcelona, C/Martí I Franquès 1, E-08028 Barcelona, Spain

Received: April 22, 2004; In Final Form: July 23, 2004

Spin polarized density functional theory based calculations within the GGA/PW91 exchange-correlation functional have been carried out to investigate the interaction of Co, Rh, and Ir atoms with the Al-terminated α -Al₂O₃(0001) surface at 1/3 ML coverage. A periodic supercell approach has been used and two possible spin states of the adsorbed metal atoms have been considered. The predicted adsorption energies follow the order Ir \approx Co > Rh and it is found that, independently of the spin state and of the relaxation of the oxide substrate, the preferred sites for the adsorption of these metals always involve interaction with surface oxygen atoms. The three transition metal atoms prefer to bind the surface at the 3-fold hollow oxygen sites although for Co the interaction on top of an oxygen adsorption site is practically equivalent. For the three transition metal atoms adsorption on top of the outermost surface aluminum atoms is clearly unfavorable. Explicit consideration of the spin polarization effects is important since Co and Ir maintain the number of unpaired electrons as in the free atoms whereas a spin quenching is observed for Rh. Metal adsorption is accompanied by some reduction of the substrate leading to a large surface relaxation mainly involving a displacement of the outermost aluminum layer.

I. Introduction

Metal deposition on surfaces constitutes one of the most useful techniques to produce modified supports with a wide variety of interesting properties.¹ This is especially the case for the activation of metal oxide surfaces because most of them, being relatively chemically inert, can be easily promoted, for instance, by deposition of alkali metals.^{2,3} Deposition of transition metals also leads to materials exhibiting modified surface properties with enormous interest in heterogeneous catalysis.⁴ Additionally, the resulting deposited particle size lies within the nanometer range exhibiting exceptional physical or chemical properties that may be of technical interest and are consequently attracting more and more attention in fundamental and applied research. One of the driving forces behind this strong interest in metal–oxide interfaces is its increasing demand in many applications ranging from metal–ceramic-based gas sensors to microelectronic devices. Therefore, it is not surprising that the physics and chemistry of the metal–oxide interface is being intensively investigated.^{5,6}

Aluminum oxide (Al₂O₃) is a particularly important substrate for catalysis due to its mechanical and thermal resistance. Metal growth on alumina surfaces has been experimentally studied by using both native surfaces of α -alumina and thin films of aluminum oxide grown on metallic substrates. The second option has the obvious advantage that scanning tunneling microscopy (STM) and electron spectroscopic techniques can be applied without charging problems although it has been very recently found that the resulting oxide thin film structure is reminiscent

of the κ -Al₂O₃ phase.⁷ Many experimental studies concerning the adsorption of transition metal atoms on oxide supports have been reported over the past few years.^{8–16} Among transition metals, Co, Rh, and Ir exhibit a well-known ability to catalyze a large number of chemical reactions when deposited on alumina.⁸

With the aim to analyze the growth and binding of metal particles on the oxide substrate a large amount of work has been carried out over the past few years. Bäumer et al.¹⁷ studied the growth of various metals, Rh, Co, and Ir, on a thin well-ordered alumina film at two different temperatures, 90 and 300 K, although due to experimental limitations the characterization of the deposits by STM was always performed at 300 K. It was shown that all metals exhibit three-dimensional growth modes irrespective of the deposition temperature and that the metal support interaction follows the Ir \approx Co > Rh > Pd trend with a concomitant increase of the overall mobility of the adsorbed metal atoms on the surface with the decreasing metal–support interaction. To obtain information about charge-transfer processes accompanying the formation of the metal–support interface Frank et al.¹⁸ vapor deposited small amounts of transition metals (Pd, Rh, and Ir) onto a thin film aluminum oxide grown on a NiAl single-crystal surface under UHV conditions and used STM to characterize the size and nucleation behavior of the metal particles, as well as using CO as a probe molecule in infrared reflection absorption spectroscopy (IRAS). The combination of STM and IRAS techniques permits one to estimate the extent of metal–oxide charge transfer for the interaction of metal particles with point defects and regular sites of the oxide substrate. For the case of Pd adsorption on alumina model substrates, it has been shown that charge transfer does not exceed $\pm 0.2e$ in agreement with previous theoretical

* Corresponding author. E-mail: sanz@us.es.

[†] Universidad de Sevilla.

[‡] Faculdade de Ciências da Universidade do Porto.

[§] Universitat de Barcelona i Parc Científic de Barcelona.

works.^{19–21} Frank et al.¹⁸ also suggest that the stronger metal–oxide bond between Rh atoms and oxide line defects is connected to the transfer of 0.5–0.6 elementary charges to the oxide.

From a theoretical point of view the adsorption of transition metals, TMs, on alumina has been rather extensively studied in the past few years, including different surface terminations (Al- or O-terminated), different surfaces models (embedded cluster or periodic supercell), and several exchange-correlation methods (Hartree–Fock or various density functional approximations).^{22–31} Whereas the study of the structure and adhesion properties of metal clusters on α -Al₂O₃(0001) is still in its infancy, a few papers have been published dealing with Pd₃ and Pd₄, and Pd₃ and Pt₃, respectively.^{32–34} For TM atoms on alumina, periodic density functional theory (DFT) calculations based on the Local Density Approximation (LDA) have been reported for the adsorption of Ag and Pt atoms on the Al-terminated α -Al₂O₃(0001) surface.²² The authors found that at low coverage Ag atoms are preferentially adsorbed above surface aluminum atoms while Pt is adsorbed above the outermost oxygen atoms. However, for a 1 ML geometrical coverage, the LDA predicts that both metals slightly prefer direct adsorption on surface aluminum atoms. Later, Bogicevic and Jennison²³ also determined the interfacial binding energies of various metals adsorbed on a alumina thin-layer film grown on Al(111) and concluded that for 1/3 ML adsorption all metals bind strongly to the oxide surface although these results refer to the oxygen-terminated surface whereas previous theoretical^{19,20} and experimental^{17,18,35,36} work correspond to the Al termination, which in UHV conditions is indeed the most stable. The nature of the interaction between Pd and α -Al₂O₃(0001) has been investigated in detail by Gomes et al.^{19,20} using embedded cluster and slab models. These authors concluded that the Pd–surface interaction arises mainly from two contributions: a polarization of the transition metal caused by the surface electrostatic field and, to a lesser extent, some charge transfer from Pd atoms toward the surface, in particular to the outermost Al atoms. The behavior described for Pd atoms on the α -Al₂O₃(0001) surface was also found for adsorbed Pt atoms and is likely to be general.²⁹ Hernández and Sanz determined surface–adsorbate and adsorbate–adsorbate pair potentials from a series of periodic DFT model calculations and used these potentials in subsequent classical molecular dynamics, MD, simulation of Pd²⁴ and Cu²⁶ particles deposition on the α -Al₂O₃(0001) surface. In the case of copper atoms,²⁵ two kinds of copper atoms were observed depending on the metal deposited coverage. At 1/3 ML, Cu atoms reduce the outermost Al ions, while increasing the coverage to 2/3 ML leads to a coexistence of Cu(I) and Cu(0), in agreement with experimental data.³⁷ Zhukovskii et al.²⁸ studied the adsorption of Ag on both Al- and O-terminated surfaces for two different metal coverages using periodic Hartree–Fock including a posteriori correction for correlation effects through an appropriate functional. In the case of the Al-terminated surface, a small adhesion energy of 0.15–0.25 and 0.40–0.55 eV has been computed for 1 and 1/3 ML coverage, respectively, and per Ag atom. The small interaction energies calculated are accompanied by minor interfacial charge transfer, most characteristic of physisorption, which may be explained by a weak atomic polarization. On the contrary, in the case of an O-terminated alumina surface much larger adhesion energies were computed, varying in the interval 3 to 11 eV taking into account 1 and 1/3 ML coverages in agreement with the work of Bogicevic and Jennison.²³ Moreover, for the O-terminated surface, noticeable charge transfer from silver atoms toward the

substrate occurs (0.5e to 0.9e) and suggests a strong interfacial ion binding. Periodic and embedded cluster DFT calculations for the coinage metals on α -alumina also show that the metal–oxide binding energies are correlated with the extent of charge transfer. Further, it was shown that Cu and Ag prefer the hollow site on aluminum ions while Au is absorbed more favorably on top oxygen atoms and that in the case of deposited Cu a clear reduction of the surface is observed. Ma et al.³⁰ investigated the adsorption of Co and Ni on the α -Al₂O₃(0001) surface using the full-potential linear-augmented plane-wave, FP-LAPW, approach and a metal coverage of 1/3 ML. They considered several different adsorption sites and concluded that Co and Ni atoms were only favorably adsorbed at 3-fold oxygen sites with interaction energies of 1.10 and 1.09 eV, respectively. In contrast with previous works, adsorption above alumina surface oxygen atoms was not energetically favorable. Further, the net spin charge density was found to reside inside the Co/Ni atomic spheres and the interstitial region and seems to be due to polarization of the metal–oxide.

This work aims to contribute to extend our knowledge of the interaction of transition metal atoms with the Al-terminated clean α -Al₂O₃(0001) surface. To this end we present a detailed theoretical study of the adsorption of Co, Rh, and Ir atoms on different sites of this surface using a periodic supercell approach based on DFT calculations within the Generalized Gradient Approximation (GGA). While, in general, nonspin polarized approaches can provide valuable insight on the metal–support interaction, explicit consideration of spin-polarization effects may be of importance as shown by recent findings.³⁸ The explicit consideration of different magnetic states represents a novelty with respect to previous works where this feature is ignored.

This paper is organized as follows: In section II, models and computational method are described. In section III, results and discussion are presented. Finally, the main conclusions are outlined in section IV.

II. Models and Computational Methods

In the present work, the repeated slab periodic approach has been employed to represent a perfect and infinite Al-terminated corundum surface and its interaction with Co, Rh, and Ir uniformly deposited at 1/3 ML coverage. Surface coverage is defined in such a way that 1 ML coverage means that 100% of the surface oxygen sites are occupied by metal atoms. The present model of the α -Al₂O₃(0001) surface is a 12-layer slab obtained by truncating the bulk α -Al₂O₃ structure leaving exposed one Al layer with an oxygen layer right beneath it, this surface termination is generally known as Al-terminated α -Al₂O₃(0001) surface. Other surface terminations are also possible but the present study will concern exclusively Co, Rh, and Ir adsorption on the Al-terminated surface since it seems established from LEED experiments that under UHV conditions this is the favored termination.³⁹ The unit cell consists of a rhombic prism belonging to the hexagonal system to which periodic 3D conditions were imposed. The lattice parameters were set to $a = b = 4.782$ Å and the c parameter was chosen in such a way that a vacuum width of 10 Å is located between the repeated slabs. This vacuum width is large enough that layer-to-layer interactions are prevented. Previous theoretical and experimental studies have indicated that the Al-terminated α -Al₂O₃(0001) surface undergoes large relaxation from its bulk structure (cf. ref 40 and references therein). The unit cell consists of 20 atoms disposed in 12 layers, both sides are Al-terminated and follow the Al–O–Al–Al–O–Al–Al–O–Al–Al–O–Al scheme. It is worth pointing out here that negligible differences

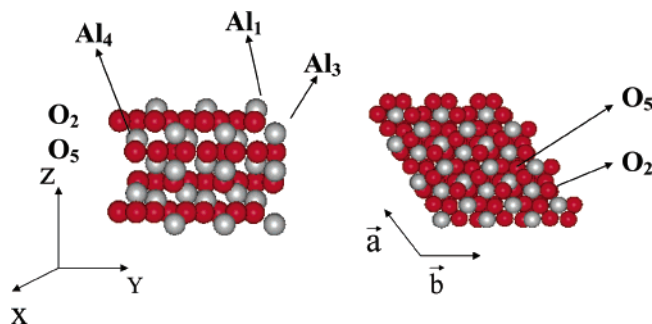


Figure 1. Schematic view of the 3D repeated slab model used to represent the Al-terminated α -Al₂O₃(0001) surface showing the adsorption sites. Red and gray spheres correspond to oxygen and aluminum atoms, respectively.

were observed between adsorption energies and geometries computed with the 12-layer unit cell or with a larger cell containing up to 30 Al and O atoms in the unit cell and 18 atomic layers.^{19,20,25}

The periodic super-cell 3D DFT calculations were carried out by using the VASP 4.6.3 code^{41–43} and the GGA implementation proposed by Perdew et al.⁴⁴ Ultrasoft pseudopotentials⁴⁵ were employed to represent the effect of core electrons on the valence shells and a plane-wave basis set was used to span the valence electronic states. The cutoff energy for the plane waves was 270 eV, and a Monkhorst–Pack set of 8 *k*-points was used. In all cases the system was partially optimized, allowing only full relaxation of the TM adatoms and of the substrate top outermost six layers. Structural optimization was performed by using a conjugated gradient technique in which the iterative relaxation of atomic positions was stopped when the change in the total energy between successive steps was less than 0.001 eV. With this criterion, forces on the atoms are generally less than 0.1 eV/Å.

Five different sites on the Al-terminated α -Al₂O₃(0001) surface were considered for Co, Rh, and Ir as shown in Figure 1, where labels Al₁ and O₂ are used to distinguish 1st-layer Al and 2nd-layer O atoms, respectively. These sites may be regarded as top sites because of the very small distance between these two atomic layers. The Al₃, Al₄, and O₅ labels refer to hollow sites with the cavity centered on an aluminum atom, of the third or fourth layers, or on an oxygen atom of the fifth layer, respectively. For the hollow sites, it is necessary to point out that this is just a labeling scheme and we do not mean that we expect a direct interaction between the TM atom and these deeply lying layers. For each site, the adsorption energy was calculated as the difference between the energy of the TM–oxide surface slab supersystem and the sum of the energies of the free Al-terminated α -Al₂O₃ surface and of that of the isolated TM atom. Since the TM atoms have open shells, spin-polarized calculations were used to compute energy differences. In any case, it is worth pointing out that obtaining the proper atomic states by means of DFT is not a simple task and usually involves a symmetry broken solution where total spatial and spin angular momentum are not well defined.^{38,46} In the present work, the energies of the isolated TM atoms were computed by placing one single atom in a 10 × 10 × 10 Å³ empty cubic box. Experimentally, it is known that *J*-averaged high spin states coming from both d⁷s² and d⁸s¹ configurations in Co and Ir atoms are close in energy⁴⁷ and, thus, nondynamical correlation effects may be of importance here. We have checked these effects by computing the energy of the isolated atoms in the high spin state for both d⁷s² and d⁸s¹ configurations and found that the GGA functional predicts the wrong configuration of

the Co and Ir atoms: d⁸s¹ instead of d⁷s².⁴⁷ However, although the computed ground state is not the experimental one, the error in the computed energy is small (less than 0.3 eV) and, in any case, will not affect the relative energies computed for the adsorption of the TM atoms on the different surface sites. Thus, in all cases, we have used as references for the isolated atom the energy computed for the high spin state coming from the experimental ground-state configuration (d⁷s² for Co and Ir, and d⁸s¹ for Rh).

Two spin states corresponding to one or three unpaired spins were considered in the computations involving Co, Rh, or Ir adsorption on the Al-terminated α -Al₂O₃(0001) surface. These different spin settings do not correspond to pure spin states although they can be regarded as reasonable estimates for the lowest doublet and quartet states of the adsorbed TM atom. It is worth pointing out that at the 1/3 ML coverage, lateral interactions among the TM atoms become a part of the adsorption energy. However, this is a small contribution for the final adsorption energy since the minimum TM–TM distance is 4.782 Å. Still, large lateral interactions will show up in case the adsorbed TM bears a noticeable charge. However, all indications in the next section strongly suggest that the net charge on the supported metal atom is small.

III. Results and Discussion

Previous works dealing with the interaction of metals on an Al-terminated α -Al₂O₃(0001) surface have established that the clean surface exhibits a very strong relaxation^{40,48} that is somehow restored upon interaction with adsorbed metal atoms.^{19,20,29,33} For the clean surface the optimum interlayer distances predicted by the present calculations are in good agreement with previous works.^{40,48} The influence of this adsorbate induced surface relaxation structural change on the energy interaction of adsorbed Co, Rh, and Ir atoms has been investigated in some detail. To this end, in the first series of calculations the oxide surface atoms were kept frozen at the positions obtained in a previous step concerning the optimization of the clean surface, and only the position of the TM atom was fully optimized. In a subsequent series of calculations, all coordinates of the adsorbed metal atom and of the six outermost oxide surface atomic layers were fully optimized. Note that the structures found in this way are just stationary points on the potential energy surfaces (PES). No vibrational analysis has been performed to characterize each one of them as minimum or saddle points. Given the close proximity of all considered adsorption sites one may expect that a lateral displacement would take the TM atom from less favorable geometries to more favorable ones. However, for the sites considered here, this cannot occur since the underlying C3 symmetry leads to a zero gradient in the direction parallel to the surface. As a consequence, the metal atom is maintained above the initial site even it is not the most stable one. The final results concerning energies and geometrical data upon adsorption of the three TM atoms initially positioned above the five regular sites on the Al-terminated α -Al₂O₃(0001) surface are reported in Tables 1, 2, and 3. These tables include results for the cases with one or three unpaired electrons on the Co, Rh, and Ir adatoms. Adsorption energies (*E*_{ads}), TM to oxide surface distance, and also the amount of relaxation of the outermost Al layer are reported. Other geometrical parameters are not given since, as in previous works^{19,20} concerning the adsorption of Pd on the Al-terminated α -Al₂O₃(0001) surface, it was revealed that the deeper oxide layers are almost unchanged when compared with their initial positions. Neglecting the adsorbate-induced surface

TABLE 1: Adsorption Energy (E_{ads}), Co to Surface Distance (Co–surf), and Outermost Al Layer Displacements (ΔAl) for Co Adsorption on the Al-Terminated $\alpha\text{-Al}_2\text{O}_3(0001)$ Surface from GGA Periodic Calculations^a

	adsorption sites				
	Al ₁	O ₂	Al ₃	Al ₄	O ₅
unrelaxed					
$-^2E_{\text{ads}}/\text{eV}$	0.89	1.80	1.63	2.04	1.66
$-^4E_{\text{ads}}/\text{eV}$	1.53	2.04	1.88	1.96	2.00
$^2d(\text{Co-surf})/\text{\AA}$	2.468	1.915	1.681	1.475	1.680
$^4d(\text{Co-surf})/\text{\AA}$	2.624	1.869	1.701	1.439	1.653
relaxed					
$-^2E_{\text{ads}}/\text{eV}$	1.12	2.90	2.42	2.90	2.09
$-^4E_{\text{ads}}/\text{eV}$	1.60	3.01	2.54	3.02	2.41
$^2d(\text{Co-surf})/\text{\AA}$	2.539	0.828	0.914	0.839	1.317
$^4d(\text{Co-surf})/\text{\AA}$	2.570	0.895	0.987	0.900	1.415
$^2\Delta\text{Al}/\text{\AA}$	0.178	0.510	0.508	0.503	0.273
$^4\Delta\text{Al}/\text{\AA}$	0.128	0.498	0.500	0.499	0.288

^a The superscripts 2 and 4 are used to distinguish from the adsorption of the metal atom in the near doublet and quadruplet states (1 or 3 unpaired electrons per metal atom, respectively).

TABLE 2: Adsorption Energy (E_{ads}), Rh to Surface Distance (Rh–surf), and Outermost Al Layer Displacements (ΔAl) for Rh Adsorption on the Al-Terminated $\alpha\text{-Al}_2\text{O}_3(0001)$ Surface from GGA Periodic Calculations^a

	adsorption sites				
	Al ₁	O ₂	Al ₃	Al ₄	O ₅
unrelaxed					
$-^2E_{\text{ads}}/\text{eV}$	1.16	1.90	1.55	1.77	1.78
$-^4E_{\text{ads}}/\text{eV}$	0.89	1.32	1.27	1.36	0.84
$^2d(\text{Rh-surf})/\text{\AA}$	2.467	1.968	1.752	1.811	1.698
$^4d(\text{Rh-surf})/\text{\AA}$	2.624	2.095	1.772	1.829	1.692
relaxed					
$-^2E_{\text{ads}}/\text{eV}$	1.22	2.34	2.16	2.13	2.52
$-^4E_{\text{ads}}/\text{eV}$	0.97	1.60	1.70	1.70	2.28
$^2d(\text{Rh-surf})/\text{\AA}$	2.453	1.626	1.113	1.545	1.150
$^4d(\text{Rh-surf})/\text{\AA}$	2.542	1.779	1.144	1.557	1.210
$^2\Delta\text{Al}/\text{\AA}$	0.210	0.315	0.505	0.277	0.660
$^4\Delta\text{Al}/\text{\AA}$	0.077	0.277	0.436	0.337	0.284

^a The superscripts 2 and 4 are used to distinguish from the adsorption of the metal atom in the near doublet and quadruplet states (1 or 3 unpaired electrons per metal atom, respectively).

relaxations one finds different preferred adsorption sites for each one of the three metal atoms.

For adsorbed cobalt, it is found that, neglecting adsorbate induced relaxation effects, the high (H) and low (L) spin states appear to be equally preferred although at different sites: E_{ads} becomes 2.04 eV for Co(L) adsorbed on Al₄ sites and for Co(H) adsorbed on O₂ sites (Table 1). A closer inspection of this table shows that for the Co(L) case the Al₄ site is clearly preferred, ca. +0.2 eV, while for Co(H) E_{ads} is about the same for both O₂ and O₅ oxygen sites and only the Al₁ site is clearly disfavored. Compared to previous results involving Pd adsorption,¹⁹ the smaller atomic radius of Co facilitates the approximation of the latter to the oxide surface although for atop adsorption both TM atoms exhibit similar distances to the surface. For all sites and electronic states, E_{ads} largely increases when the six outermost layers of the oxide surface are allowed to relax although now the Co(H) is always favored. The adsorbate induced surface relaxation causes large distortion of the substrate with a concomitant increase in the adsorption energy that ranges from 0.23 to 1.1 eV (leading to E_{ads} values of ~ 3.0 eV) depending on the adsorption site. In fact, this enhancement of the interaction is almost due to the induced outward relaxation of the outermost aluminum atoms that, recovering some lost coordination with respect to the bulk, tend to restore the

TABLE 3: Adsorption Energy (E_{ads}), Ir to Surface Distance (Ir–surf), and Outermost Al Layer Displacements (ΔAl) for Ir Adsorption on the Al-Terminated $\alpha\text{-Al}_2\text{O}_3(0001)$ Surface from GGA Periodic Calculations

	adsorption sites				
	Al ₁	O ₂	Al ₃	Al ₄	O ₅
unrelaxed					
$-^2E_{\text{ads}}/\text{eV}$	0.83	1.83	2.07	1.30	1.48
$-^4E_{\text{ads}}/\text{eV}$	1.36	1.64	1.41	1.67	0.83
$^2d(\text{Ir-surf})/\text{\AA}$	2.534	1.892	1.786	1.723	1.878
$^4d(\text{Ir-surf})/\text{\AA}$	2.655	2.117	1.892	1.788	1.892
relaxed					
$-^2E_{\text{ads}}/\text{eV}$	1.12	2.80	2.07	2.55	2.10
$-^4E_{\text{ads}}/\text{eV}$	1.58	2.10	2.23	2.65	3.17
$^2d(\text{Ir-surf})/\text{\AA}$	2.492	1.080	0.960	1.066	1.529
$^4d(\text{Ir-surf})/\text{\AA}$	2.517	1.724	1.107	1.034	1.635
$^2\Delta\text{Al}/\text{\AA}$	0.310	0.535	0.609	0.623	0.439
$^4\Delta\text{Al}/\text{\AA}$	0.280	0.320	0.570	0.540	0.440

^a The superscripts 2 and 4 are used to distinguish from the adsorption of the metal atom in the near doublet and quadruplet states (1 or 3 unpaired electrons per metal atom, respectively).

interlayer distance. The overall effect is of course somewhat unlikely when Co atoms are placed right above surface Al₁ atoms and explains why only in this case is the adsorption energy less affected. For the other surface sites it is found that substrate relaxation is smaller in the case of the O₅ site and this is consistent with a smaller variation in the adsorption energy. This is also in agreement with a decrease in the interlayer displacements found for the clean oxide surface when it is cut from bulk alumina.^{40,48} However, this interpretation is in contradiction with the strong induced relaxation effects found for Rh adsorption on the O₅ site and irrespective of the spin state; this point will be further discussed below. Ma et al.³⁰ have studied the adsorption of Co on the alumina surface with a six layer model in which only the three outermost layers were allowed to relax and the Perdew–Burke–Ernzerhof (PBE) implementation of the GGA exchange–correlation functional. These authors have also explicitly considered spin polarization and found that the high spin case is preferred as in the present calculations. They found that only the 3-fold oxygen site (Al₄ in this paper) was favorable for Co adsorption on alumina. This finding is in clear contradiction with the present results reported for Co and also for Rh and Ir and with several previous theoretical works devoted to the adsorption of other TM atoms on the same oxide surface.^{19,20,22,28} Very recently, the PBE and PW91 GGA exchange–correlation functionals were used to obtain knowledge about the formation of Frenkel defects on both bulk and surface alumina.⁴⁸ Identical results were obtained with these two exchange–correlation functionals and, hence, the different adsorption energies obtained by Ma et al. have to be attributed to a number of factors: the use of a too limited slab used to model the alumina surface; the lack of relaxation on deeper layers; the spin state of the isolated metal atom not being defined. The two first factors are important because the final adsorption energy will be affected by any difference in the relaxation of the bare surface and in the one taking into account the adsorbate induced relaxation. It is very possible that both effects are differently affected by decreasing the number of atomic layers. These differences may explain why the E_{ads} values reported by Ma et al. for Co on $\alpha\text{-Al}_2\text{O}_3(0001)$ are nearly 50% of the present values.

Let us now consider the case of adsorption of Rh atoms on the relaxed corundum surface (Table 2). Three main differences are evidenced when compared to Co adsorption on the same oxide substrate. First, the adsorption energies for both the frozen and the induced relaxed surfaces are somewhat smaller than

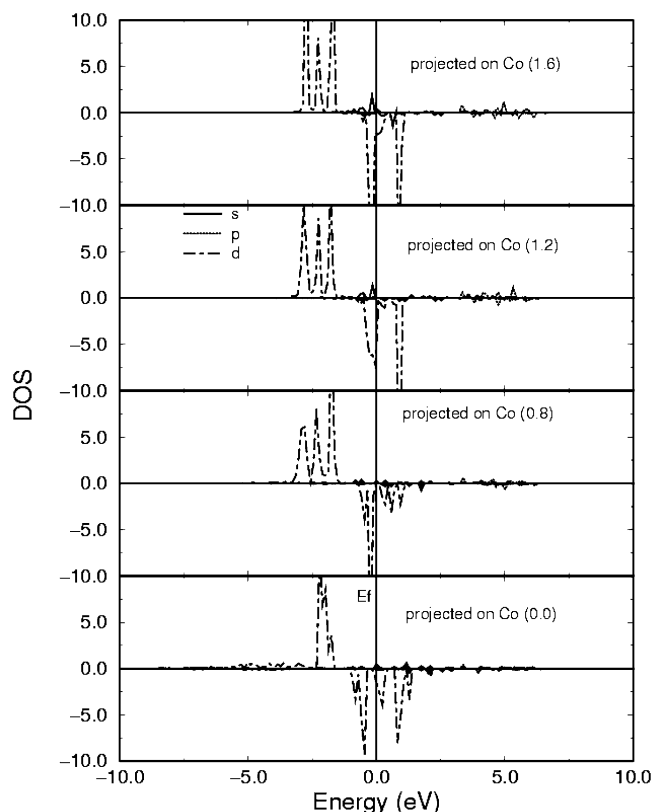


Figure 2. GGA projected density of states for 1/3 ML of cobalt adsorbed on the Al₄ site of the α -Al₂O₃(0001) surface for optimized structure (0.0) and increasing the *z* coordinate by 0.8, 1.2, and 1.6 Å. The calculations have been performed for the high spin state (\sim Co quartet) of the system.

that for Co. Second, Rh atoms are always preferentially adsorbed in the low spin state. And finally, that adsorption above oxygen atoms (O₂ and O₅) is preferred: the most favorable situation after surface relaxation involving interaction with the O₅ site in the low spin state with $E_{\text{ads}} = 2.52$ eV. Yet a different behavior is found for the adsorption of Ir atoms which are found to prefer the low spin state if the surface is frozen and the high spin state if adsorbate induced relaxation effects are taken into account (Table 3) thus showing the importance of taking into account both spin polarization and adsorbate induced relaxation effects, simultaneously. In fact, it appears that the degree of surface relaxation is related to the spin state of the adsorbed TM atom. In the case of the frozen substrate, Ir(H) adsorption on the Al₁ site is almost as favorable as adsorption on the other sites, which was not the case for the other two metal atoms considered in the present work. When the six outermost Al and O layers are allowed to relax, the adsorption above oxygen atoms is preferred with calculated adsorption energies of 3.17 eV on O₅ for the high spin state compared to only 2.80 eV for the most favorable adsorption site (O₂) if the low spin state is considered. Notice that the change in the preferred spin state when induced relaxation is considered occurs for Ir but not for Co and Rh. Finally, the data reported in Tables 1–3 show that these three TM atoms avoid adsorption at the surface directly on top of aluminum positions (Al₁) and prefer to lie close to the oxygen sites, above or on hollow sites, independently of the spin state and surface relaxation being considered or not.

The adsorbate induced surface relaxation can be interpreted as a purely coordination effect although chemical reduction of the surface may also play a role. A rigorous evaluation of the amount of charge transfer between the TM and the oxide surface can be carried out by making use of modern methods of

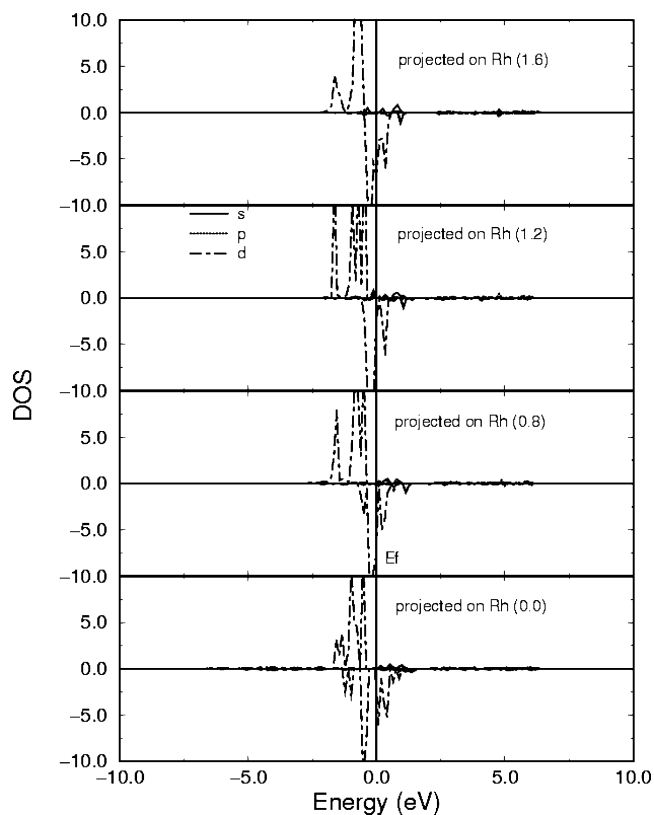


Figure 3. GGA projected density of states for 1/3 ML of rhodium adsorbed on the O₅ site of the α -Al₂O₃(0001) surface for optimized structure (0.0) and increasing the *z* coordinate by 0.8, 1.2, and 1.6 Å. The calculations have been performed for the low spin state (\sim Rh doublet) of the system.

topological analysis such as aim or ELF as was done recently for TM atoms on various oxide surfaces.²¹ However, this requires the use of a cluster model with the concomitant problems arising from a complex and strongly relaxed surface. This is because the numerical integration of the electron density on the topologically defined atomic volume cannot be carried out with the present plane wave based computational codes. A qualitative description of the charge transfer between the TM and the oxide surface can be investigated with the help of the projected density of states (DOS) curves, and electron-density maps. This analysis was performed for adsorption on the most favorable sites only and considering the relaxed systems. The projected DOS computed at the optimized TM–oxide surface distance are reported in Figures 2, 3, and 4 for Co, Rh, and Ir atoms, respectively. For the sake of comparison, the projected DOS obtained when the TM atom is displaced along the *z* coordinate by +0.8, +1.2, and +1.6 Å are also included in these figures. A close inspection of Figure 2 shows that no *s* band appears in the DOS projected on the Co atom at the optimized geometry. However, when the Co atom is displaced away from the surface a small *s* peak is clearly observed near E_{f} . This band is also noticed for Ir adsorption but its intensity is smaller than that of Co. In the case of Rh adsorption, the *s* band is observed only when the TM atom has been displaced by 1.6 Å. The results coming from the DOS features, Figures 2–4, combined with those given in Tables 1–3 suggest that Co and Ir are preferentially adsorbed in a high spin d^7s^2 configuration while Rh is adsorbed in a d^9s^0 configuration and hence necessarily low spin. These findings suggest that upon adsorption the TM atoms experience at least some electron rearrangement or hybridization together with some surface reduction.

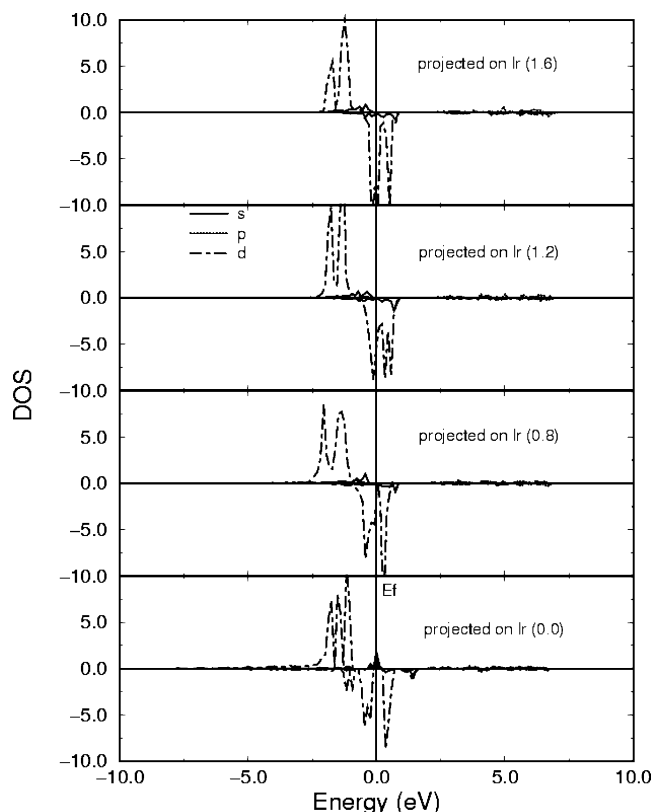


Figure 4. GGA projected density of states for 1/3 ML of iridium adsorbed on the O₅ site of the α -Al₂O₃(0001) surface for optimized structure (0.0) and increasing the *z* coordinate by 0.8, 1.2, and 1.6 Å. The calculations have been performed for the high spin state (\sim Ir quartet) of the system.

With the aim to go one step further in the understanding of the charge-transfer process that takes place upon TM atoms deposition on the alumina surface, maps corresponding to the difference in the electron density, $\Delta\rho = \rho(M/\alpha\text{-Al}_2\text{O}_3) - \rho(\alpha\text{-Al}_2\text{O}_3) - \rho(M)$, are depicted in Figure 5. These maps show a clear reorganization of the electron density around the TM atom that can be interpreted as a d to s hybridization. At the same time the electron density rises in the regions near the outermost Al atoms, mainly for Rh and Ir adsorption, and near surface oxygen atoms the electron density increases only slightly. The overall balance between electron density gain and loss is very difficult to establish although one can infer a small but noticeable reduction of the oxide surface. On the basis of not only on the electron density maps of Figure 5, but also on the DOS presented in Figures 2–4, we may infer that there is some electron rearrangement on the adsorbed TM atom together with some, but small, surface reduction. Such a surface reduction also agrees with both experimental data reported for Pd, Rh, and Ir by Frank et al.¹⁸ and theoretical results concerning Pd,^{19,20} Cu,²⁵ and Au²⁶ deposition.

Finally, to analyze the bonding between the three TM atoms and the oxide surface at the most stable sites, the projected DOS on the TM, Al, and O atoms are represented in Figures 6, 7, and 8. In all cases the α component of the calculated DOS projected on aluminum and oxygen atoms shows clear asymmetric peaks corresponding to the *p* sites. These peaks arise from the hybridization with the TM *d* band and, consequently, illustrate the importance of the orbital mixing in the metal–support interaction. The DOS projected on Al at energies higher than *E_f* and the DOS projected on O at an energy around -20 eV reveal a clear different behavior depending on the TM atom

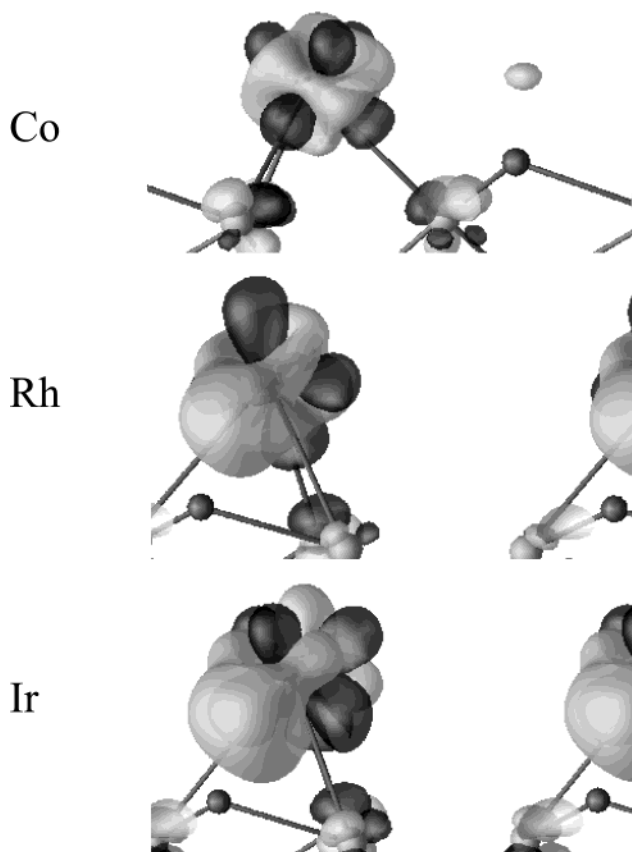


Figure 5. Calculated electron-density differences for 1/3 ML of Co, Rh, and Ir adsorbed on the α -Al₂O₃(0001) surface. Dark and light gray represent density difference isosurfaces corresponding to -1.4 cell volume \times electron/Å³ (electron energy loss with respect to the separated systems) and 1.4 cell volume \times electron/Å³ values (electron energy gain with respect to the separated systems). Top: Co/ α -Al₂O₃ on the Al₄ site. Middle: Rh/ α -Al₂O₃ on the O₅ site. Bottom: Ir/ α -Al₂O₃ on the O₅ site.

deposited and show some substrate induced electronic reorganization upon metal deposition.

To summarize, we may try to rationalize the behavior of the three TM atoms from the picture that emerges after analyzing the ensemble of results presented. All three metals prefer anion sites to interact with the surface: in the case of Co directly atop on an O₂ site and a hollow site, O₅, both for Rh and Ir. This is probably due to the lower atomic radius of the Co atom (1.25 Å) when compared to the Rh or Ir atoms (1.34 and 1.36 Å) that allows a close proximity to the anion and, thus, a stronger interaction. In all three cases the interaction energy is high, around 3 eV for Co and Ir, and slightly less, 2.5 eV, for Rh. From the DOS curves and the data in Tables 1–3 it results that Co and Ir prefer the high spin state when adsorbed in the oxide surface while the Rh atom prefers the low spin one. One is tempted to interpret these data in terms of slightly different bonding mechanisms. For the Co atom the main contribution to the bonding will be the charge transfer to the surface together with a repolarization of the d-shell, which results from the close proximity of the atom that allows a more efficient charge-transfer mechanism. In the case of Rh and Ir, the main contribution to the bonding will be the polarization of the TM atom, as suggested by the data in Figure 5. This mechanism will be more efficient for a more polarizable atom such as Ir. This would result in a stronger interaction energy that will indeed be even larger on hollow sites, where the adatom interacts directly with three surface anions. Clearly, a deeper look at the

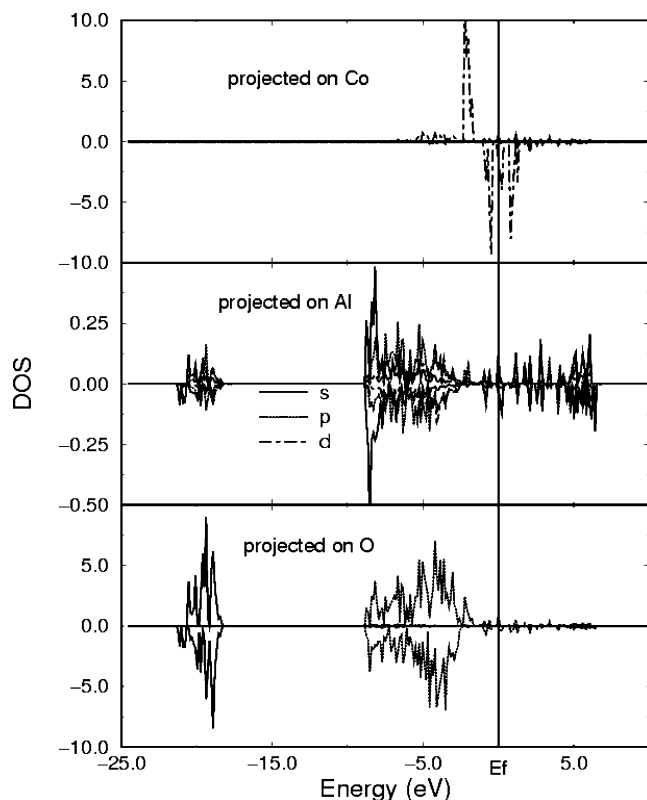


Figure 6. Calculated high spin state GGA DOS for 1/3 ML of cobalt deposited on the Al₄ site of the α -Al₂O₃(0001) surface. Top: projected on cobalt. Middle: projected on aluminum. Bottom: projected on oxygen.

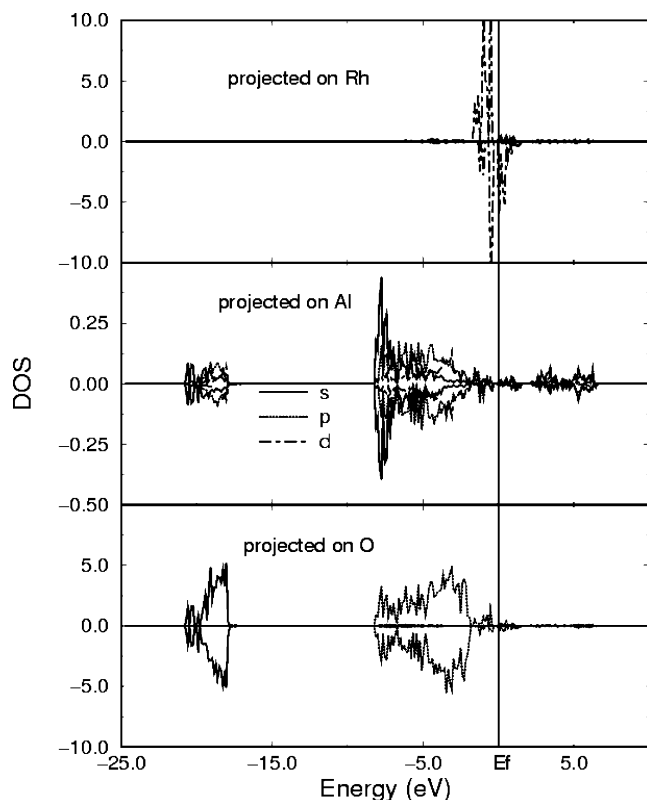


Figure 7. Calculated high spin state GGA DOS for 1/3 ML of rhodium deposited on the O₅ site of the α -Al₂O₃(0001) surface. Top: projected on rhodium. Middle: projected on aluminum. Bottom: projected on oxygen.

electronic structure of the adsorbed adatoms and their bonding is desirable as is currently under way in our laboratories.

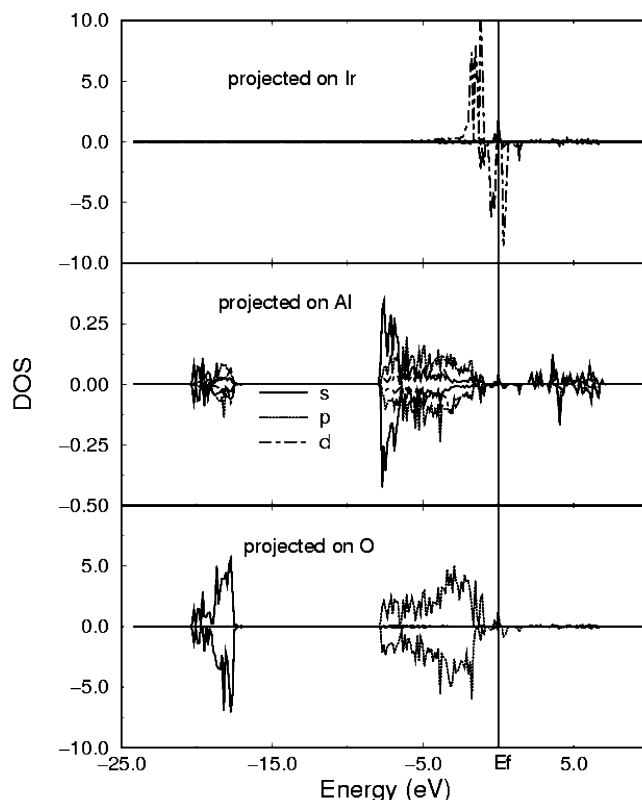


Figure 8. Calculated high spin state GGA DOS for 1/3 ML of iridium deposited on the O₅ site of the α -Al₂O₃(0001) surface. Top: projected on iridium. Middle: projected on aluminum. Bottom: projected on oxygen.

IV. Conclusions

In this work, a slab periodic model has been used to study the interaction of Co, Rh, and Ir atoms on the Al-terminated α -Al₂O₃(0001) surface at 33% coverage. The adsorption energies and equilibrium geometries were obtained from DFT calculations within the GGA method. The adsorption energies were found to vary in the order Ir \approx Co > Rh, which is in close agreement with previous experimental results reported by Bäumer et al.¹⁷ In general, Co, Rh, and Ir atoms prefer to be adsorbed close to surface oxygen atoms and this was found to be independent of the spin state considered in the calculations. However, explicit consideration of the spin polarization is important because the interaction of the TM atom with the substrate may have important effects on its local electronic state. In fact, Co and Ir are found to maintain three unpaired electrons as in the isolated atoms whereas in the case of Rh a partial quenching of the total spin is observed. Therefore, although nonspin polarized approaches can provide valuable qualitative information of the metal–support interaction, the accurate description of the interaction of TM atoms with ceramic supports requires explicit consideration of the spin polarization effects. This is in agreement with recent findings³⁸ and contrary to the common practice.

As found previously for the adsorption of other TM atoms on the corundum surface,^{19,22,24,25} the deposition of Co, Rh, and Ir atoms induces a strong relaxation of the substrate with the outermost Al atoms suffering a significant outward displacement. This may be interpreted as an effect of the recovered coordination of the outermost Al layer and also as caused by a partial reduction of the substrate surface during the TM deposition. Nevertheless, the analysis of the calculated density of state curves and difference density maps shows only a small

charge transfer between the oxide and the adsorbed TM atoms in the case of Co and Ir, which contrasts with the behavior found for Rh adsorption. These findings are in agreement with previous experimental results reported by Frank and co-workers.¹⁸

Acknowledgment. Financial support from the Spanish Ministerio de Ciencia y Tecnología (projects BQU2002-04029-C02-01, MAT2002-0756 and the Ramon y Cajal program (awarded to N.C.H.)), Junta de Andalucía (FQM-132), and Generalitat de Catalunya (projects 2001SGR-00043 and Distinció de la Generalitat de Catalunya per a la Promoció de la Recerca Universitària awarded to F.I.) is fully acknowledged. J.R.B.G. thanks the Fundação para a Ciência e a Tecnologia, FCT, Lisbon, Portugal, for the award of a post-doc scholarship (SFRH/BPD/11582/2002). Computer time was in part provided by the Centre de Supercomputació de Catalunya, CESCA, Centre Europeu de Paral·lelisme de Barcelona, CEPBA, and CEBPA-IBM-Research Institute, CIRI, through generous grants from Universitat de Barcelona, Fundació Catalana per a la Recerca and CIRI.

References and Notes

- (1) Henrich V. E.; Cox, P. A. *The surface science of metal oxides*; Cambridge University Press: Cambridge, U.K., 1994.
- (2) Sordelli, L.; Guidotti, M.; Andreatta, D.; Vlais, G.; Psaro, R. *J. Mol. Catal. A: Chem.* **2003**, *204*, 509.
- (3) Lemonidou, A. A.; Nalbandian, L.; Vasalos, I. A. *Catal. Today* **2000**, *61*, 333.
- (4) Henry, C. R. *Surf. Sci. Rep.* **1998**, *31*, 231.
- (5) Gates, B. C. *Chem. Rev.* **1995**, *95*, 511.
- (6) Goodman, D. W. *Chem. Rev.* **1995**, *95*, 523.
- (7) Stierle, A.; Renner, F.; Streitel, R.; Dosch, H.; Drube, W.; Cowie B. C. *Science* **2004**, *12*, 1652.
- (8) Bäumer, M.; Freund, H.-J. *Prog. Surf. Sci.* **1999**, *61*, 127.
- (9) Bäumer, M.; Frank, M.; Libuda, J.; Stempel, S.; Freund, H.-J. *Surf. Sci.* **1997**, *391*, 204.
- (10) Frank, M.; Andersson, S.; Libuda, J.; Stempel, S.; Sandell, A.; Brena, B.; Gierzt, A.; Brühwiler, P. A.; Bäumer, M.; Artensson, N.; Freund, H.-J. *Chem. Phys. Lett.* **1997**, *279*, 92.
- (11) Chen, J. G.; Crowell, J. E.; Yates, J. T., Jr. *Surf. Sci.* **1987**, *187*, 243.
- (12) Regalbutto, J. R.; Navada, A.; Shadid, S.; Bricker, M. L.; Chen, Q. *J. Catal.* **1999**, *184*, 335.
- (13) Chen, D. A.; Bartelt, M. C.; Seutter, S. M.; McCarty, K. F. *Surf. Sci.* **2000**, *464*, L708.
- (14) Serna, R.; Afonso, C. N.; Ricolleau, C.; Wang, Y.; Zheng, Y.; Gandais, M.; Vickridge, I. *Appl. Phys. A* **2000**, *71*, 583.
- (15) Kim, Y. D.; Wei, T.; Wendt, S.; Goodman, D. W. *Langmuir* **2003**, *19*, 7929.
- (16) Judai, K.; Abbet, S.; Worz, A. S.; Heiz, U.; Giordano, L.; Pacchioni, G. *J. Phys. Chem. B* **2003**, *107*, 9377.
- (17) Bäumer, M.; Frank, M.; Heemeier, M.; Kühnemuth, R.; Stempel, S.; Freund, H.-J. *Surf. Sci.* **2000**, *454–456*, 957.
- (18) Frank, M.; Bäumer, M.; Kühnemuth, R.; Freund, H.-J. *J. Phys. Chem. B* **2001**, *105*, 8569.
- (19) Gomes, J. R. B.; Illas, F.; Hernández, N. C.; Márquez, A.; Sanz, J. *F. Phys. Rev. B* **2002**, *65*, 125414.
- (20) Gomes, J. R. B.; Illas, F.; Hernández, N. C.; Sanz, J.; Wander, A.; Harrison, N. M. *J. Chem. Phys.* **2002**, *116*, 1684.
- (21) Gomes, J. R. B.; Illas, F.; Silvi, B. *Chem. Phys. Lett.* **2004**, *388*, 132.
- (22) Verdozzi, C.; Jennison, D. R.; Schultz, P. A.; Sears, M. P. *Phys. Rev. Lett.* **1999**, *82*, 799.
- (23) Bogicevic, A.; Jennison, D. R. *Phys. Rev. Lett.* **1999**, *82*, 4050.
- (24) Hernández, N. C.; Sanz, J. F. *J. Phys. Chem. B* **2001**, *105*, 12111.
- (25) Hernández, N. C.; Sanz, J. F. *J. Phys. Chem. B* **2002**, *106*, 11495.
- (26) Hernández, N. C.; Sanz, J. F. *Appl. Surf. Sci.* In press.
- (27) Hernández, N. C.; Sanz, J. *THEOCHEM*. In press.
- (28) Zhukovskii, Y. F.; Kotomin, E. A.; Herschend, B.; Hermansson, K. P.; Jacobos, W. M. *Surf. Sci.* **2002**, *513*, 343.
- (29) Rivanenkov, V. V.; Nasluzov, V. A.; Shor, A. M.; Neyman, K. M.; Rösch, N. *Surf. Sci.* **2003**, *525*, 173.
- (30) Ma, Q.; Klier, K.; Cheng, H.; Mitchell, J. W.; Hayes, K. S. *J. Phys. Chem. B* **2001**, *105*, 2212.
- (31) Jennison, D. R.; Mattson, T. R. *Surf. Sci. Lett.* **2003**, *544*, L689.
- (32) Gomes, J. R. B.; Lodziana, Z.; Illas, F. *J. Phys. Chem. B* **2003**, *107*, 6411.
- (33) Lodziana, Z.; Nørskov, J. K. *Surf. Sci.* **2002**, *518*, L577.
- (34) Nasluzov V. A.; Rivanenkov V. V.; Shor A. M.; Neyman, K. M.; Rosch N. *Chem. Phys. Lett.* **2003**, *374*, 487.
- (35) Frank, M.; Kühnemuth, R.; Bäumer, M.; Freund, H.-J. *Surf. Sci.* **2000**, *454–456*, 968.
- (36) Frank, M.; Bäumer, M. *Phys. Chem. Chem. Phys.* **2000**, *2*, 3723.
- (37) Kelber, J. A.; Niu, C.; Shepherd, K.; Jennison, D. R.; Bogicevic, A. *Surf. Sci.* **2000**, *446*, 76.
- (38) Markovits, A.; Paniagua, J. C.; López, N.; Minot, C.; Illas, F. *Phys. Rev. B* **2003**, *67*, 115417.
- (39) Toofan, J.; Watson, P. R. *Surf. Sci.* **1998**, *401*, 162.
- (40) Gomes, J. R. B.; Moreira, I. P. R.; Reinhardt, P.; Wander, A.; Searle, B.; Harrison, N. M.; Illas, F. *Chem. Phys. Lett.* **2001**, *341*, 412 and references therein.
- (41) Kresse, G.; Hafner, J. *Phys. Rev. B* **1993**, *47*, 558.
- (42) Kresse, G.; Furthmüller, J. *Comput. Mater. Sci.* **1996**, *6*, 15.
- (43) Kresse, G.; Furthmüller, J. *Phys. Rev. B* **1996**, *54*, 11169.
- (44) Perdew, J.; Chevary, J.; Vosko, S.; Jackson, K.; Pederson, M.; Singh, D.; Fiolhais, C. *Phys. Rev. B* **1992**, *46*, 6671.
- (45) Vanderbilt, D. *Phys. Rev. B* **1990**, *41*, 7892.
- (46) Baerends, E. J.; Branchadell, V.; Sodupe, M. *Chem. Phys. Lett.* **1997**, *265*, 481.
- (47) Sansonetti, J. E.; Martin, W. C.; Young, S. L. *NIST Handbook of Basis Atomic Spectroscopic Data* (<http://physics.nist.gov/PhysRefData/Handbook/index.html>).
- (48) Carrasco, J.; Gomes, J. R. B.; Illas, F. *Phys. Rev. B* **2004**, *69*, 064116.